Empowering the crowd: Feasible strategies to minimize the spread of COVID-19 in high-density informal settlements

Alberto Pascual-García[1,*], Jordan Klein[2], Jennifer Villers[3,∧],
Eduard Campillo-Funollet[4,∧], Chamsy Sarkis[5]

February 15, 2021

(1) Institute of Integrative Biology. ETH-Zürich. Zürich, Switzerland.
(2) Office of Population Research. Princeton University. Princeton, NJ, USA.
(3) Princeton Environmental Institute. Princeton University. Princeton, NJ, USA.
(4) Genome Damage and Stability Centre. University of Sussex. Brighton, United Kingdom.
(5) Pax Syriana Foundation. Valetta, Malta.
(∧) Equal contribution.
(*) correspondence: alberto.pascual@env.ethz.ch

Abstract

More than 1 billion people live in informal settlements worldwide, where precarious living conditions pose unique challenges to managing a COVID-19 outbreak. Taking Northwest Syria as a case-study, we simulated an outbreak in high-density informal Internally Displaced Persons (IDP) camps using a stochastic Susceptible-Exposed-Infectious-Recovered model. Expanding on previous studies, taking social conditions and population health/structure into account, we modeled several interventions feasible in these settings: moderate self-distancing, self-isolation of symptomatic cases, and protection of the most vulnerable in "safety zones". We considered complementary measures to these interventions that can be implemented autonomously by these communities, such as buffer zones, daily health-checks, and carers for isolated individuals, quantifying their impact on the micro-dynamics of disease transmission. All interventions significantly reduce outbreak probability and mortality. Self-distancing reduces mortality by up to 35% if contacts are reduced by 50%. A similar reduction in mortality can be achieved by providing 1 self-isolation tent per 200 people. Protecting the most vulnerable in a safety zone has synergistic effects with the other interventions and reduces mortality in the most vulnerable population. Our model predicts that a combination of all simulated interventions may reduce mortality by as much as 80% and delay an outbreak's peak by more than three months. Our results highlight the potential for non-medical interventions to mitigate the effects of the pandemic. Similar measures may be applicable to controlling COVID-19 in other informal settlements, particularly IDP camps in conflict regions, around the world.

Key questions

What is already known?

- Since the onset of the COVID-19 pandemic, many studies have provided evidence for the effectiveness of strategies such as social distancing, testing, contact tracing, case isolation, use of personal protective equipment/facemasks and improved hygiene to reduce the spread of the disease. These studies underlie the recommendations of the World Health Organisation, but their implementation is contingent on local conditions and resources.

- Mathematical modelling is the basis of many epidemiological studies and has helped inform policymakers considering COVID-19 responses around the world. Nevertheless, only a limited number of studies have applied these models to informal settlements.

What are the new findings?

- We developed a mathematical model to study the dynamics of COVID-19 in Syrian IDP camps, elaborating on previous efforts done in similar settings by explicitly parametrizing the camps' demographics, living conditions and micro-dynamics of interpersonal contacts in our modelization.

- We designed interventions such as self-distancing, self-isolation and the creation of safety zones to protect the most vulnerable members of the population, among others, through conversations with camp managers with on-the-ground knowledge of what interventions would be feasible and have community buy-in.

- Our results show how low-cost, feasible, community-led non-medical interventions can significantly mitigate the impact of COVID-19 in Northwest Syrian IDP camps.

What do the new findings imply?

- Our model represents a step forward in the much-needed search for epidemiological models that are sufficiently flexible to consider specific social questions. The model can also help inform similar interventions in refugee camps in conflict-torn regions, and potentially be adapted to other informal settlements and vulnerable communities around the world.

Introduction

The COVID-19 pandemic is intensifying in regions immersed in protracted armed conflicts [1], where large portions of their populations have become displaced. When the displaced population exceeds official resettlement and refugee camp capacity, Internally Displaced Persons (IDPs) must live in informal settlements (hereafter named "camps"). These regions must contend with the public health challenges resulting from violence [2], the deterioration of health-systems [3], especially of critical care [4], and the breakdown of essential public infrastructure such as water and sanitation systems [5]. Urgent action is needed to contain the virus in these settings, a task which necessarily involves the engagement of the communities living in them [6].

This study focuses on the Northwest region of Syria (NWS): a relatively small geographical area with 4.2 million people, of which 1.15 million (27.4%) are IDPs living in camps [7], and where the number of cases increased twenty-fold between September 8th and October 20th, 2020 [8]. The health status of households in camps in NWS is poor; 24% have a member with a chronic disease, of whom 41% have no access to medicines [9]. As in other conflict regions, the political instability in NWS hinders coordinated public health actions, and the ongoing movements of IDPs create ample opportunity for infectious disease transmission, while making contact tracing interventions infeasible.

To investigate feasible COVID-19 prevention interventions in the camps, we considered a Susceptible-Exposed-Infectious-Recovered model similar to the one presented in [10], in which the camps' populations are divided into classes reflecting their estimated age-structures and comorbidity prevalence. We use this model to propose various interventions aimed at reducing the number of contacts within and between population classes in general, and with symptomatic individuals in particular. We paid special attention to how the living conditions in informal camps inform the assumptions underlying our proposed interventions, a question often neglected [11]. We modeled interventions previously proposed for African cities [12], such as self-distancing, isolation of symptomatic individuals and the creation of a 'safety zone' in which more vulnerable members of the population are protected from exposure to the virus.

Building upon the approach used to model the impact of these interventions in African cities, our model includes a parameterization of the contacts each individual has per day [12]. We further elaborate upon this approach by making a more explicit representation of contacts and other parameters in the model. We consider the micro-dynamics of contacts, the time that individuals take to recognize their symptoms before self-isolating, the effect of having carers to attend to isolated individuals, and the existence of a buffer zone in which exposed and protected population classes can interact under certain rules. We examine a potential worst-case scenario in which there is no access to any healthcare facility. Since empowering local communities in conflict regions to understand how to control COVID-19 is possibly the most (and perhaps only) effective way to minimize its spread, our models are of utmost importance for informing the implementation of realistic interventions in these regions.

Methods

The model

We consider a model simulating a viral outbreak in a single camp over a 12-month period inspired by those proposed by [10] [13] (see Fig. 1). The model is adapted to the context of NWS IDP camps and is divided into compartments containing individuals at different possible stages along the disease's progression, governed by the following set of differential equations:

$$\dot{S}_i = -\lambda_i S_i \tag{1}$$

$$\dot{E}_i = \lambda_i S_i - \delta_{\mathrm{E}} E_i \tag{2}$$

$$\dot{P}_i = \delta_{\mathrm{E}} E_i - \delta_{\mathrm{P}} P_i \tag{3}$$

$$\dot{A}_i = (1-f)\delta_{\mathrm{P}} P_i - \gamma_{\mathrm{A}} A_i \tag{4}$$

$$\dot{I}_i = f\delta_{\mathrm{P}} P_i - (l_i \gamma_I + h_i \eta + g_i \alpha) I_i \tag{5}$$

$$\dot{H}_i = h_i \eta I_i - \gamma_{\mathrm{H}} H_i \tag{6}$$

$$\dot{R}_i = \gamma_{\mathrm{A}} A_i + l_i \gamma_I I_i + (1-\sigma)\gamma_{\mathrm{H}} H_i \tag{7}$$

$$\dot{D}_i = g_i \alpha I_i + \sigma \gamma_{\mathrm{H}} H_i \tag{8}$$

The susceptible population (S_i) becomes exposed at rate λ_i, while exposed individuals (E_i) progress through the latent period at rate δ_{E} to a preclinical infectious stage (P_i), which then progresses to (at rate δ_{P}) either a a clinical (symptomatic, I_i, with probablity f) or subclinical (asymptomatic, A_i, with probability $1-f$) infectious stage. Asymptomatic cases recover (R_i) at rate γ_{A}. Symptomatic cases have 3 potential outcomes: mild cases will recover at rate γ_I, severe cases will progress to an extended infectious period during which they require hospitalization (H_i) at rate η, while critical cases requiring ICU care will die (D_i) at rate α. Finally, since the fate of individuals in the hospitalized compartment is uncertain if healthcare is not available, we run simulations considering two possibilities: either all recover ($\sigma = 0$), or all die ($\sigma = 1$) (see section Epidemiological severity assumptions). The specific values for the parameters are presented in Table 1.
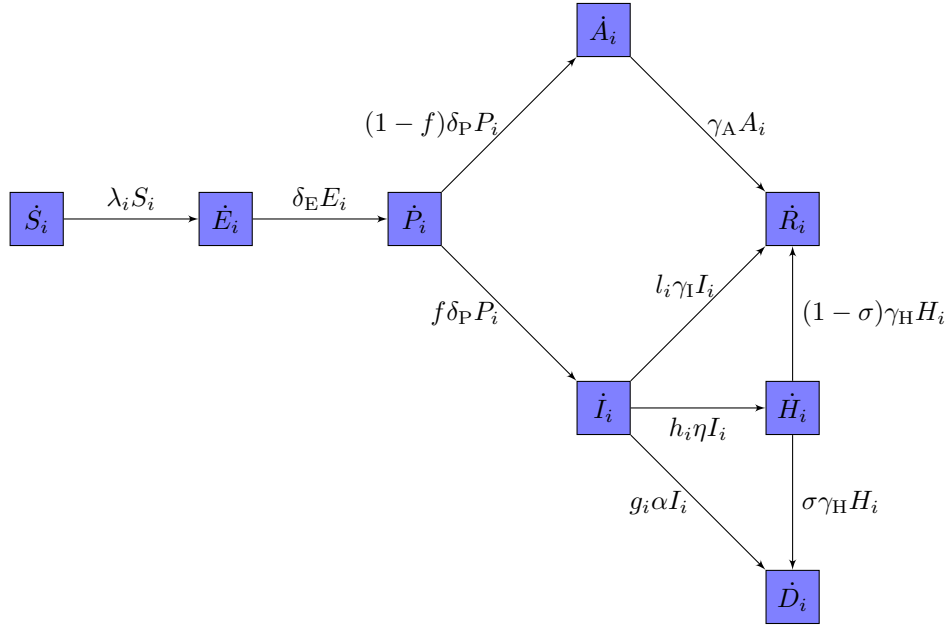

Figure 1: **Diagram of the model.** The model considers the following compartments: susceptible (S), exposed (E), infectious-presymptomatic (P), infectious-asymptomatic (A), infectious-symptomatic (I), infectious-requiring hospitalization (H), recovered (R) and dead (D).

The model splits the population into classes (indexed i) to account for heterogeneity with respect to clinical risk and behaviour. Working with population classes allows us to encode behavioural assumptions in the model and strike an appropriate balance between generality, computational tractability, and the requisite specificity to realistically evaluate our proposed interventions [14]. Moreover, the explicit representation of contacts between and within population classes allows us to design interventions considering cultural and context-specific assumptions [11] (see section Interventions and Supplementary Material for details). Under a null model where no interventions are implemented, the distinctions between classes are only dependent on age and comorbidity status (hereafter "demographic-classes"). h_i, g_i and l_i are demographic-class specific parameters, adjusted to ensure that the

proportions of symptomatic cases progressing through each of the 3 potential clinical outcomes (mild, severe, and critical) are consistent with the literature (see section Epidemiological severity assumptions).

Under some interventions, the demographic-classes may be subdivided further into subclasses according to behaviour ("behaviour-classes"). Consequently, different interventions may require models with different numbers of classes. We refer to both demographic- and behaviour-classes generically as "classes" (see section Interventions for the modelization of behaviour-classes).

Parameter	Description	Value	Distribution	Reference
$1/\delta_{\mathrm{E}} + 1/\delta_{\mathrm{P}}$	Incubation period (days)	5.2 (95% CI: 4.1-7.0)	Lognormal	[15]
$1/\delta_{\mathrm{P}}$	Presymptomatic infectious period (days)	2.3 (95% CI: 0.8-3.8)	Gaussian	[16, 17]
$1/\delta_{\mathrm{E}}$	Latent period (days)	$(1/\delta_{\mathrm{E}} + 1/\delta_{\mathrm{P}}) - 1/\delta_{\mathrm{P}}$ (Minimum = .5 days)		Derived
$1/\gamma_{\mathrm{I}}$	Symptomatic infectious period (days)	7	---	[16, 18]
$1/\gamma_{\mathrm{A}}$	Asymptomatic infectious period (days)	7	---	[16, 18]
$1/\eta$	Time from symptom onset to requiring hospitalization (days)	7 (IQR: 4-8)	Gamma	[19]
$1/\alpha$	Time from symptom onset to death (critical cases, days)	10 (IQR: 6-12)	Gamma	[19]
$1/\gamma_{\mathrm{H}}$	Time from requiring hospitalization to recovery/death (days)	10 (IQR: 7-14)	Gamma	[19]
f	Probability an infectious individual is symptomatic	0.84 (95% CI: 0.8-0.88)	Binomial	[20]
σ	Indicator of whether hospitalized recover or die	$\sigma \in \{0,1\}$	---	Assumed
τ	Maximum transmissibility	0.14 (95% CI: 0.05-0.40)	Lognormal	Derived
β_{P}	Presymptomatic transmissibility relative to τ	Reference stage (=1)	---	[21, 17]
β_{A}	Asymptomatic transmissibility relative to τ	0.14 (95% CI: 0.05-0.40)	Lognormal	Derived
β_{I}	Clinical symptomatic transmissibility relative to τ	0.24 (95% CI: 0.11-0.60)	Lognormal	Derived
β_{H}	Hospitalized transmissibility relative to τ	0.11 (95% CI: 0.05-0.29)	Lognormal	Derived

Table 1: **Fixed parameters.** See Methods and Supplementary Materials for details.

Transmissibility assumptions

Although individuals in IDP camps share tents with other co-occupants, whom they may be more likely to infect than occupants of different tents, we ignore spatial structure in our model and assume a well-mixed population. This is justified because individuals from different tents share common spaces (e.g. letrines) and have frequent interactions, in particular kids. Consequently, our following derivation of the transmissivity parameter itself, τ, is not spatially explicit.

The rate at which susceptible individuals become exposed is

$$\lambda_i = \sum_{j=1}^{n} \tau C_{ij} \frac{\beta_{\mathrm{P}} P_j + \beta_{\mathrm{A}} A_j + \beta_{\mathrm{I}} I_j + \beta_{\mathrm{H}} H_j}{N_j}, \tag{9}$$

5

where C_{ij} is the average number of contacts that individuals of class i have with individuals of class j per day and N_j is the total population size of class j. We parametrized C_{ij} by multiplying the mean number of total contacts that individuals from a population class i have per day, c_i, by the probability of random interaction with individuals of class j. Considering a well-mixed population, this probability is proportional to class j's fraction of the total population, i.e. $C_{ij} = c_i N_j/N$. If interventions are absent, we consider demographic-classes only and, hence, different values of c_i reflect heterogeneity in the number of contacts by age group. We assume specific values of c_i for each class based on conversations with camp managers in NWS (see Table 2).

The probability of infection if there is a contact between a susceptible and an infected person is $\tau\beta_{\mathrm{P}}$, $\tau\beta_{\mathrm{A}}$, $\tau\beta_{\mathrm{I}}$ or $\tau\beta_{\mathrm{H}}$ depending upon whether the infected individual is in the presymptomatic (P_i), symptomatic (I_i), asymptomatic (A_i), or hospitalized compartment (H_i), respectively. The τ parameter is the maximum transmissivity, which is observed at the presymptomatic stage [16]. Thus, we selected the presymptomatic stage as a reference ($\beta_{\mathrm{P}} = 1$) with the remaining β parameters set relative to β_{P} ($\beta_i < \beta_{\mathrm{P}}$, $i \in \{\mathrm{A}, \mathrm{H}, \mathrm{I}\}$) (see Table 1, Supplementary Materials for derivation).

The τ parameter was estimated by randomly generating a value for the basic reproduction number, R_0, following a Gaussian distribution with a mean of 4 (99% CI: 3–5) and dividing this value by the the dominant eigenvalue of the Next Generation Matrix (see section Computational implementation for details and Supplementary Material for the analytical results). The distribution of R_0 was a compromise between values reported in the literature from regions with high-density informal settlements: R_0=2.77 in Abuja and 3.44 in Lagos, Nigeria [22], 3.3 in Buenos Aires [23], and 5 in Rohingya refugee camps in Bangladesh [24].

Population structure of demographic-classes

We parameterized the model with data from IDPs in NWS [25]. The population sizes of informal camps are approximately log-normally distributed, with a mean of of 1212. We simulated camps with populations of 500, 1000 and 2000 individuals. Since interventions tend to be less effective in larger camps, the results presented refer to simulations with 2000 individuals, unless otherwise specified. For our demographic-classes, we considered 3 age groups: children (age 1, 0-12 years old), younger adults (age 2, 13-50 yrs) and older adults (age 3, >50 yrs). For ages 2 and 3, we considered two subclasses comprising healthy individuals and individuals with comorbidities (see Table 2).

Parameter	Description	Demographic-class					References
		Age 1 (0-12)	Age 2 (13-50) no comorbidities	Age 2 (13-50) comorbidities	Age 3 (>50) no comorbidities	Age 3 (>50) comorbidities	
Fraction in class	–	0.407	0.471	0.0626	0.022	0.0373	[25, 26]
c_i	Mean contacts per day	25	15	15	10	10	From camp managers

Table 2: **Demographic class-specific parameters.** Estimated proportions of individuals in the population and mean number of contacts per individual per day for each demographic class. See Supplementary Materials for derivactions.

Epidemiological severity assumptions

In NWS, there are 4 active and 2 planed COVID-19 referral hospitals, with a current capacity of 66 ventilators, 74 ICU beds and 355 ward beds for 4.2 million people [27, 28]. Estimations based on an exponential growth model from Hariri et al. predicted a collapse of health facilities 8 weeks into an outbreak [29]. Although we do not have access to official data on healthcare occupancy, the currently reported number of cases suggests that this scenario could already have been reached [8]. Hence, we considered a worst-case scenario in which individuals will not have access to healthcare and assumed that all critical cases (those requiring ICU care) would die. However, there is greater uncertainty about the fate of severe cases, those requiring hospitalization but not ICU care. We therefore considered a compartment for severe cases to account for a longer infectious period if they stay in the camp (see compartment H_i, Fig. 1). This compartment also helped us model some interventions more realistically, for example by noting that the symptoms of severe cases are incompatible with self-isolation. To estimate upper and lower bounds for the outcome variables of our model, we simulated two possible scenarios for the fate of this

Parameter	Description	Demographic class				
		Age 1 (0-12)	Age 2 (13-50) no comorbidities	Age 2 (13-50) comorbidities	Age 3 (>50) no comorbidities	Age 3 (>50), comorbidities
q_i^{H} (h_i)	Fraction of symptomatic cases severe	0.064 (0.064)	0.067 (0.066)	0.199 (0.191)	0.183 (0.178)	0.445 (0.406)
q_i^{D} (g_i)	Fraction of symptomatic cases critical	0.0065 (0.009)	0.020 (0.028)	0.094 (0.129)	0.063 (0.088)	0.222 (0.289)

Table 3: **Proportion of clinical symptomatic cases resolving into severe and critical cases.** Since the rates at which these cases resolve into these three epidemiological outcomes is different, we introduced three parameters (h_i, g_i and l_i) to distribute individuals according to the desired proportions (values between parenthesis). The proportion of individuals recovering is computed as $1 - q_i^{\mathrm{H}} - q_i^{\mathrm{D}}$ (see Supplementary Materials for details).

compartment: one in which all cases recover, and another in which all die. In the simulations presented in the Main Text, we consider the worst-case scenario in which all of these cases die.

The fractions of symptomatic cases that are severe (q_i^{H}), critical (q_i^{D}) and recover (q_i^{R}, where $q_i^{\mathrm{R}} = 1 - q_i^{\mathrm{H}} - q_i^{\mathrm{D}}$) are demographic-class-specific (see Table 3). We estimated the fractions of symptomatic cases in each demographic-class that would become severe (q_i^{H}) and critical (q_i^{D}) using data from developed countries with superior population health [30, 31]. Following previous work [12], we mapped the age-specific case severity distributions of the NW Syrian adult population to those of 10 years older age groups in developed countries.

Since the rates at which clinical symptomatic individuals (I_i) resolve into these three epidemiological outcomes is different (η for H, α for D and γ_{I} for R) we introduced three parameters, h_i, g_i and l_i, to distribute individuals according to the desired proportions
. The analytic solution is provided in Suppl. Material and the specific values in Table 3.

Computational implementation

We considered a continuous-time Markov process with discrete variables, in which individuals jump from one epidemiological compartment to another with instant transition rates determined by Eqs. 1–8. The specific values of the parameters shown in these equations and of R_0 are independently drawn at each integration step from the probability distributions shown in Tables 1, 1 and 2. The Next Generation Matrix is also computed at each integration step from the parameters drawn, and τ is then estimated. To ensure computational efficiency, all these random values are precalculated. In the code provided it is possible to fix the seed to exactly reproduce the results presented. The equations are then integrated with a Gillespie algorithm implemented in the adaptivetau package [32] in R [33]. Our simulations start with a completely susceptible population where one person in the younger adult population is exposed to the virus. We verified that a steady state was always reached before the end of each simulation. We did not consider migration, births, nor deaths due to other causes, since they are small enough in magnitude to not significantly impact the course of an outbreak, provided additional conflict does not erupt.

Interventions

The interventions we are considering influence population's behaviour, and are modelled modifying the rate at which individuals become exposed (the term λ_i, Eq. 9). Since λ_i can be factorized in four terms, the interventions may influence one or several of these terms. The factors present in λ_i and the terms modulating them in the interventions are (see Eq. 10): i) the maximum transmissibility, τ, which is reduced in some interventions by a factor ξ, when interactions are restricted to buffer zones (see below for details); ii) the average number of contacts that individuals in class i have per day, c_i. This quantity can either be reduced (e.g. self-isolation) or contacts be unevenly distributed depending on which class j interacts with class i (e.g. whether the two classes live in the same zone in the camp, which help us to implicitly encode simple spatial structures). In its more general form, these type of interventions can be modelled introducing a factor ϵ_{ij} multiplying c_i; iii) the probability of encountering between a member of class i and members of class j in a well-mixed population, N_j/N, can either be
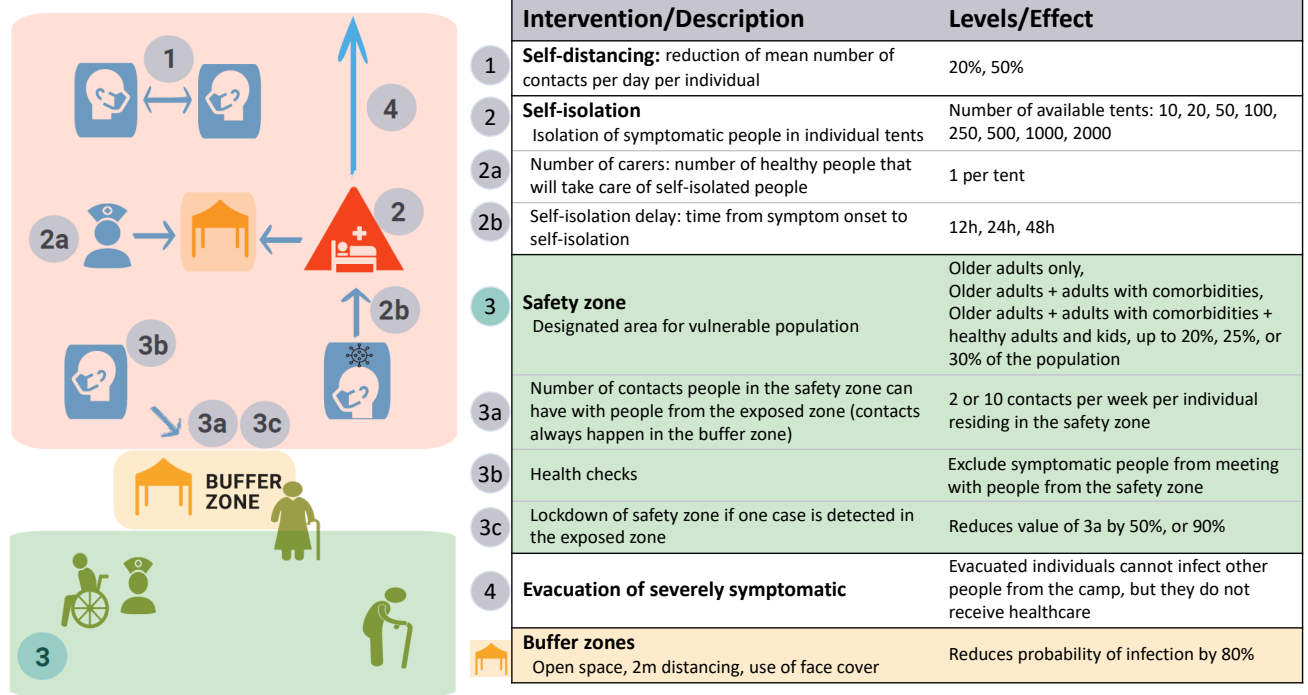
	Intervention/Description	Levels/Effect
1	**Self-distancing:** reduction of mean number of contacts per day per individual	20%, 50%
2	**Self-isolation** Isolation of symptomatic people in individual tents	Number of available tents: 10, 20, 50, 100, 250, 500, 1000, 2000
2a	Number of carers: number of healthy people that will take care of self-isolated people	1 per tent
2b	Self-isolation delay: time from symptom onset to self-isolation	12h, 24h, 48h
3	**Safety zone** Designated area for vulnerable population	Older adults only, Older adults + adults with comorbidities, Older adults + adults with comorbidities + healthy adults and kids, up to 20%, 25%, or 30% of the population
3a	Number of contacts people in the safety zone can have with people from the exposed zone (contacts always happen in the buffer zone)	2 or 10 contacts per week per individual residing in the safety zone
3b	Health checks	Exclude symptomatic people from meeting with people from the safety zone
3c	Lockdown of safety zone if one case is detected in the exposed zone	Reduces value of 3a by 50%, or 90%
4	**Evacuation of severely symptomatic**	Evacuated individuals cannot infect other people from the camp, but they do not receive healthcare
	Buffer zones Open space, 2m distancing, use of face cover	Reduces probability of infection by 80%

Figure 2: **Diagram of interventions.**

increased or reduced (e.g. safety zone, isolation) by introducing a factor ω_{ij}; and iv) the probablility of becoming infected by individuals at specific stages of the disease, e.g. for hospitalized individuals this is encoded in the term $\beta_{\mathrm{H}} H_j / N_j$, can also be modified by specific factors. Only the terms for individuals at the clinical symptomatic (I) and hospitalized (H) stages are modified in our interventions, through the parameters ζ_{I} and ζ_{H}, respectively. Following these considerations, the generic form of λ_i under the interventions becomes:

$$\lambda_i = \underbrace{\tau\xi}_{i} \sum_{j=1}^{n} \underbrace{c_i \epsilon_{ij} \omega_{ij}}_{ii} \underbrace{\frac{N_j}{N}}_{iii} \underbrace{\left(\frac{\beta_{\mathrm{P}} P_j + \beta_{\mathrm{A}} A_j + \zeta_{\mathrm{I}} \beta_{\mathrm{I}} I_j + \zeta_{\mathrm{H}} \beta_{\mathrm{H}} H_j}{N_j} \right)}_{iv}, \tag{10}$$

where the above classification of the different factors is indicated. All interventions can be modelled following this expression, except for the self-isolation intervention which will require further adjustments to dynamically control for the proportion of population isolated in each class (see below). The specific values of the parameters are presented in Table 4 and their derivations in Supplementary Materials.

Self-distancing

The first non-medical intervention that we modeled is a reduction in the mean number of contacts per individual per day for the whole camp population (see Fig. 2-1). The average number of contacts of each class c_i (see Table 2) is reduced a fraction that is independent of the class, hence the matrix ϵ_{ij} is uniform for all classes, i.e. $\epsilon_{ij} = \epsilon, \quad \epsilon \in \{0.2, 0.5\}$. No further adjustments are required for this intervention. Since the mean number of inhabitants per tent in a camp is 5.5 and sanitation facilities are shared [25], we inferred that the number of contacts per day cannot be reduced by more than 50% ($\epsilon = 0.5$). For a younger adult, this would mean 7.5 contacts per day.

Self-isolation

Self-isolation is a challenge in informal settlements, where households consist of a single (often small) space, water is collected at designated locations, sanitation facilities are communal and food supplies are scarce. We

Intervention	ϵ_{ij}	ω_{ij}	ζ_I	ζ_H	ξ	Details
Self-distancing	$\epsilon \quad \in \{0.2, 0.5\}$	1	1	1	1	constant $\forall i, j$
Self-isolation	$(c_{\text{care}}/c_i)(\tilde{I}_j/N_{\text{exp}})$	N/N_j	1	1	0.2	$i \in$ young healthy adults $j \in$ isolated individuals in class j
	$1-(c_{\text{care}}/c_i)(\tilde{I}_j/N_{\text{exp}})$	1			1	$i \in$ young healthy adults $j \in$ individuals not isolated in class j
	0	0			0	$i \notin$ young healthy adults $j \in$ isolated individuals in class j
	1	1			1	$i \notin$ young healthy adults $j \in$ individuals not isolated in class j
Safety zone	$\vartheta c_{\text{visit}}/c_i$	N/N_Y	{0,1} see (*)	{0,1} see (*)	0.2	$i \in$ zone X, $j \in$ zone Y ($X, Y \in$ {green, orange})
	$1 - \vartheta c_{\text{visit}}/c_i$	N/N_X	1	1	1	$i, j \in$ zone X ($X \in$ {green, orange})
Evacuation	1	1	1	0	1	–

Table 4: **Parameterization of the interventions.** Values of ϵ_{ij}, ω_{ij}, ζ_I, ζ_H and ξ considered in the interventions (see Supplementary Materials for their derivations). c_{care} = number of carers out of the N_{exp} available (non-infected younger and healthy adults). $\tilde{I}_j$ = Number of isolated cases of class j. c_{visit} = maximum number of contacts that individuals in the green zone can have with individuals from the orange zone per week ($c_{\text{visit}} = \{2, 10\}$). ϑ = fraction of the population in the orange (green) zone in contact with individuals from the green (orange) zone. $\vartheta = 1$ if the class i is in the green zone, and it is proportional to $c_{\text{visit}}N_g/N_o$ if it is in the orange zone. N_X and N_Y generically refer to the total population in either the green (N_g) or the orange (N_o) zones. Note (*): The parameters ζ_I and ζ_H are set to 0 if in the intervention health checks are considered to access to the buffer zone, and set to 1 otherwise.

considered the possibility of those showing symptoms self-isolating in individual tents in dedicated parts of the camps. We simulated this intervention with various numbers of isolation tents per camp, ranging from 10 to 2000 for a camp of 2000 people (see Fig. 2-2). In addition, we modeled the role of carers dedicated to providing for isolated individuals (see Fig. 2-2a). Carers belong to the younger adults class with no comorbidities, while isolated individuals belong to any class, except the youngest population (0-12 yrs.) for which we do not consider realistic their self-isolation. Hence, the parameters ϵ_{ij} and ω_{ij} depend not only on the classes i and j but also on whether the interaction is with the specific sub-population of symptomatic infectious individuals or not and if these individuals are isolated, which depends on the isolation capacity (see Table 4). This requires controlling during the simulation if the capacity is reached and adjusting λ_i accordingly (see Supplementary Materials for the final expression for λ_i).

In addition, interactions between carers and isolated individuals were restricted to *buffer zones*, which we envisioned as open spaces, with guidelines in place to limit occupancy to 4 individuals wearing masks, with 2 meters separating individuals, where the probability of transmission is reduced by 80% ($\xi = 0.2$). In considering one carer per isolated individual with one contact per day, we do not neglect their probability of infecting the rest of the camp. We also considered minimum time intervals for individuals to recognize their symptoms: with means of 12, 24 and 48 hours (see Fig. 2-2b), which was implemented incorporating an additional compartment (O_i) between the presymptomatic (P_i) and clinical symptomatic (I_i) compartments (see Suppl. Fig. 1).

Safety zone

In this intervention, the camp is divided in two areas: a safety zone, in which more vulnerable people live (hereby referred to as a "green" zone following previous studies [12]), and an exposed ("orange") zone with the remaining population. In our simulations, the first exposed individual always belongs to the orange zone. The living conditions within both zones remain the same, so the overall contact rate does not change unless self-distancing is also implemented. A consequence of maintaining the overall contact rate is that, reducing contacts with individuals living in a different zone, implies an increase in contacts with individuals in the same zone (see Supplementary Material). Although we do not expect this assumption to be true in general, it allows us to investigate undesired side-effects of this intervention, such as older adults having increased contacts amongst themselves if isolated together. Since proposals for partitioning the population may be received differently across camps, we considered several scenarios for allocating a camp population to the two zones (see Fig. 2-3). In some of these scenarios, implementing this intervention requires the split of some demographic-classes into behaviour-classes. For example, if some healthy younger adults are allocated into the green zone, we split the demographic-class "healthy younger adults" into "orange" and "green" behaviour-classes, to model the different contacts that these two subclasses of healthy younger adults will have between them and with other classes. In Supplementary Table 2 we present the classes considered in each scenario.

Interactions between the two zones are limited to a buffer zone, reducing the transmissivity (i.e. $\xi = 0.2$, see previous section). Individuals in the green zone cannot leave and thus need to be provided with supplies by individuals in the orange zone, which will take place in the buffer zone. In our simulations, we considered limiting individuals in the green zone to 10 or 2 contacts with individuals from the orange zone per week (see Fig. 2-3a). The intervention considers that the average number of contacts per day that each class has remains the same, but that these contacts are distributed depending on whether they interact with individuals of the same or of a different zone (controlled by ϵ_{ij}) and also the probability of interaction between classes is modulated by the split in the camp (ω_{ij}, see Table 4 for specific values). Other variations of this intervention we explored include preventing symptomatic individuals from entering the buffer zone (see Fig. 2-3b) and a "lockdown" of the green zone, where the number of weekly contacts in the buffer zone is reduced by 50% or 90% (see Fig. 2-3c).

Evacuation

The last intervention we simulated is the evacuation of severe cases (individuals in the hospitalization compartment). Since they require more intensive care that cannot be delivered while adhering to the guidelines of a buffer zone, severe cases were assumed to be fully infectious and not able to self-isolate. Once severe cases are evacuated, their infectivity is reduced to zero ($\zeta_H = 0$, see Fig. 2-4). The fate of severe cases is not altered by this intervention since we assumed that hospitals are saturated and that evacuees are transferred to isolation centers instead.

Key variables and statistical analysis

For each implementation of the interventions, we ran [Review: 500] simulations and compared results between them. The main variables considered are the fraction of simulations in which at least one death is observed, a proxy for the probability of an outbreak, the fraction of the population that dies and the time until the symptomatic population peaks, as well as the infection fatality rate (IFR), the fraction of the population that recovers and the fraction of the population that remains susceptible at steady-state. For consistency, we only considered simulations in which there was an outbreak when comparing the outcome of a variable between interventions. We used the Shapiro-Wilk test [34] to verify that our results do not exhibit normally distributed residuals, Kruskal-Wallis test for pairwise comparisons [35], and Conover-Iman test for multiple comparisons [36]. We used the R package PMCMRplus [37]. Confidence intervals for the probability of outbreak were computed with Wilson's method [38] implemented in the R package binom [39]. The model and all statistical analyses were implemented in R [33];

Results

In the absence of interventions, the mean IFR is ~2% in simulations where all severe cases requiring hospitalization recover (see Supplementary Fig. 2), and ~11% in simulations where all severe cases die. We consider the latter scenario to evaluate the effect of non-medical preventive interventions. In this scenario, the probability of observing

an outbreak is close to 0.85, in which ~10% of the camp dies, the number of symptomatic cases peaks after 55 days and ~84% of the population recovers.

Self-distancing

Our results show that self-distancing has a notable effect on reducing the probability of an outbreak: a 20% reduction in daily contacts is associated with a ~10% decrease in outbreak probability (see Fig. 3A). A greater reduction in daily contacts, of 50%, is required to observe a significant decrease in mortality, of as much as 35% (see Fig. 3B). Self-distancing also significantly extends the time until the peak of the outbreak, from 55 days when there is no intervention to 110 days when contacts are reduced by 50% (see Fig. 3C). However, the proportion of the population recovered after 12 months is reduced by ~30% (see Supplementary Fig. 3).

Self-isolation

With only 10 tents for a camp of 2000 people (i.e. 1 tent for every 200 people), self-isolation yields a modest decrease in the probability of observing an outbreak (see Fig. 3D), but a stronger reduction in mortality (~30%) (see Fig. 3E). Further increasing the number of tents significantly augments this reduction until there is 1 per every 20 people (Kruskal-Conover post-hoc-test, p-val$< 3 \times 10^{-5}$). However, mortality begins to slightly increase again after this threshold. This effect and the increase in the probability of observing an outbreak are consequences of having one carer per individual isolated (see Supplementary Material), so when the isolated (infected) population increases, the number of healthy younger adults in contact with them increases in tandem. Similarly, we observe a reduction in IFR when increasing the number of tents up to 1 per every 20 people, and no significant reduction over that number (see Supplementary Fig. 4). Importantly, the potential reductions in overall fatalities and IFR from self-isolation are realized whether the time required for individuals to recognize their symptoms is 12h or 24h on average, but the intervention becomes less effective when this time increases to 48h (see Supplementary Fig. 5).

Safety zone

In this section, we consider the scenario in which all older adults, younger adults with comorbidities and their family members up to 20% of the camp population live in the green zone, unless otherwise specified. Creating a green zone improves the effect of the previous interventions overall, but with sometimes opposite outcomes in the exposed and protected populations. For example, the probability of an outbreak sharply decreases for the protected population, by almost 40%, if only two contacts are allowed per week in the buffer zone (see Fig. 3G). Notably, most of this reduction is only achieved when health-checks excluding symptomatic individuals from the buffer zone are in place (see Supplementary Fig. 7). On the other hand, the probability of an outbreak may slightly increase for the exposed population, a consequence of the relative increase in intra-zone contacts. Despite this side-effect, by shifting the burden of an outbreak towards the less vulnerable population in the orange zone, this intervention not only reduces fatalities among the more vulnerable population in the green zone (Kruskal-Wallis test, p-val$< 10^{-15}$; see Supplementary Fig. 8), but also reduces the overall IFR (see Supplementary Fig. 9) and thus the number of fatalities globally (see Fig. 3H). Another important outcome of this intervention is the notable increase in time until the number of symptomatic cases peaks for the vulnerable population (see Fig. 3I).

Considering different scenarios for allocating people to the green zone, the lowest probability of an outbreak is achieved when only older adults or at most older adults and younger adults with comorbidities move there (see Supplementary Fig. 10). Positive effects of the green zone intervention are even more marked in camps with smaller populations, for every outcome of interest except time until symptomatic cases peak (see Supplementary Fig. 11). The incorporation of a lockdown has the greatest effect on reducing the probability of an outbreak in the green zone, to under 0.10 when contacts in the buffer zone are reduced by 90%. While lockdowns show no positive effect on green zone fatalities in the few instances where an outbreak does reach there, they decrease IFR and overall fatalities by further concentrating outbreaks in the less vulnerable population (see Supplementary Fig. 12).

Evacuation

We observe no significant effects when severe cases requiring hospitalization are evacuated (see Supplementary Fig. 6). Since we considered that these individuals will not receive health care (they are evacuated to isolation
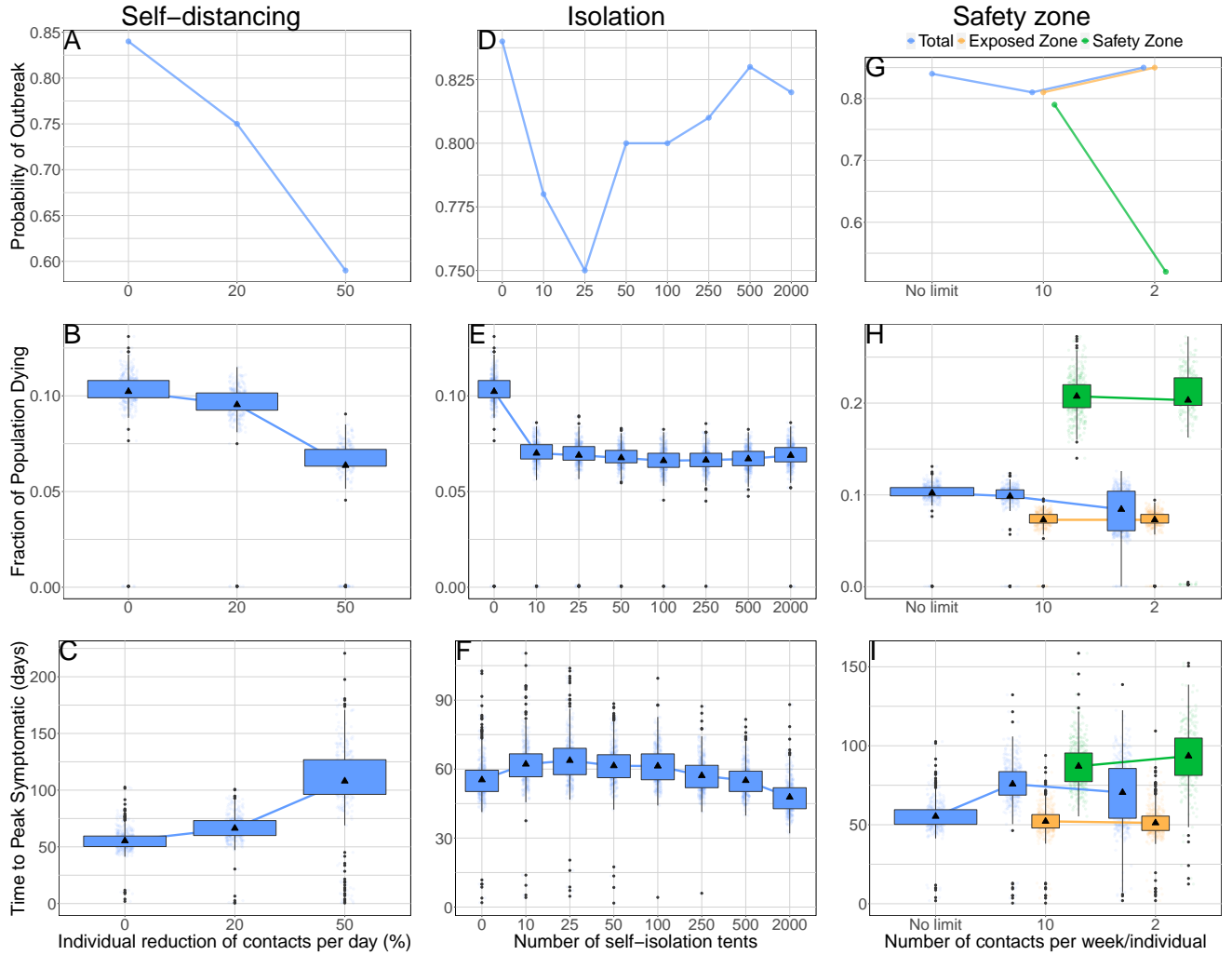
Figure 3: **Effect of interventions on outbreak probability, fatalities and time until symptomatic cases peak.** A: Self-distancing, probability of an outbreak. B: Self-distancing, fraction of the population dying. C: Self-distancing, time until peak symptomatic cases. D: Self-isolation, probability of an outbreak. E: Self-isolation, fraction of the population dying. F: Self-isolation, time until peak symptomatic cases. G: Safety zone, probability of an outbreak. H: Safety zone, fraction of the population dying. I: Safety zone, time until peak symptomatic cases. Note that in figures of the safety zone intervention (panels G-I), the mean of an outcome for the whole population is not the weighted mean of the exposed and safety zones, since outcomes are computed considering simulations in which at least one death was observed in the population class inhabiting the zone. This explains why in panel I there is a reduction in the mean time until symptomatic cases peak when moving from 10 to 2 contacts per week for the whole population, despite there being an increase in the safety zone: in ~35% of simulations there is an outbreak in the orange zone but not in the green zone (panel G).

centers), their fate remains the same than if staying in the camp and, hence, we expect evacuation to have an effect only in reducing the infectivity. Although these individuals spend a longer period being infectious with respect to an individual having mild symptoms ($\sim$10 days longer), the number of individuals under these conditions is only a small fraction of the total infectious population at any given time, what explains why we do not observe significant effects for this intervention.

Combined interventions

The effects of the interventions observed when we examine them individually build upon each other when multiple interventions are implemented in tandem (see Fig. 4 and Supplementary Fig. 13). The protective effects of the safety zone intervention especially are most fully realized not when implemented on its own, but when paired with other interventions. They become so effective that outbreaks in the green zone become exceptionally rare, but so well controlled when they do happen, that the majority of outbreaks see fewer than 20 cases. This leads to an anomalous increase in IFR in some of the most effective interventions, driven by the discretization of the values it can take (Supplementary Table. 3). When all interventions are implemented together: strict self-distancing (50% reduction in contacts), self-isolation of symptomatic cases (1 tent for every 40 people), a safety zone with 2 contacts per week in the buffer zone, health checks, a strict lockdown (90%), and evacuation of severe cases, mortality is reduced by $\sim$80%.

Discussion

In this study, we propose a number of interventions of immediate applicability to informal settlements. We focused on IDP settlements in NW Syria, taking into account the interventions' feasibility, cultural acceptance and their need for low-cost. When confronted with different possible scenarios, we generally considered the worst-cases, highlighting the interventions that are most effective in the direst conditions, but possibly resulting in an overestimate of mortality. This potential overestimation does not change the qualitative picture of the results, which is built upon comparison of relative values between the presence and absence of interventions.

Our results align with previous simulation studies of potential COVID-19 interventions in similarly densely populated, low-resource settings where informal settlements are present, such as urban areas of sub-Saharan Africa. In these settings, social-distancing is demonstrated to be an effective intervention, and even small changes are estimated to have large effects on outbreaks [40], in some cases determining whether or not already inadequate healthcare systems become overwhelmed [41]. Zandvoort et al. show that similar measures to the ones we consider: self-isolation, physical distancing and "shielding" the vulnerable, may reduce mortality by 60%-75% in African cities [12].

Self-distancing proves to be an effective measure in our models as well; reducing contacts by 50% has the greatest effect across most outcomes of interest in any of the interventions we examined. However, the difficulty of achieving a reduction of this magnitude cannot be overlooked, especially considering the large proportion of the population composed of children, a group with an already high contact rate that may prove difficult to control [25].

We also propose self-isolation using individual tents which can be located in a dedicated zone or next to the tents of relatives, where contact with non-isolated individuals is mediated by a buffer zone. This intervention is effective with even a small number of isolation tents, as low as 5-10 tents per 1000 camp residents. After conversations with camp managers, we found that this intervention is more likely to be accepted in NW Syria than evacuation to community-based isolation centers. Community-based isolation not only poses cultural challenges; the capacity required to implement it has hardly been met [28], and it is still one of the main challenges in the region [8].

One of the key parameters we assessed for the implementation of self-isolation is the need for carers. In considering one carer per isolated individual, with daily contact in a buffer zone, once a certain threshold of isolated cases ($\sim$200 per camp of 2000) is surpassed, the benefits of isolation begin to be outweighed by an increase in infectivity resulting from a growing number of exposed carers. This pitfall could be circumvented through the creation of a more organized, dedicated group of carers, thus reducing the number of healthy younger adults in contact with isolated (infectious) individuals.

Much of the success or failure of the safety zone intervention hinges on the functioning of the buffer zone. The number of inter-zone contacts per week, the implementation of health checks, and potential lockdowns all have notable effects. Also important is the portion of the population that is protected; protecting only the vulnerable
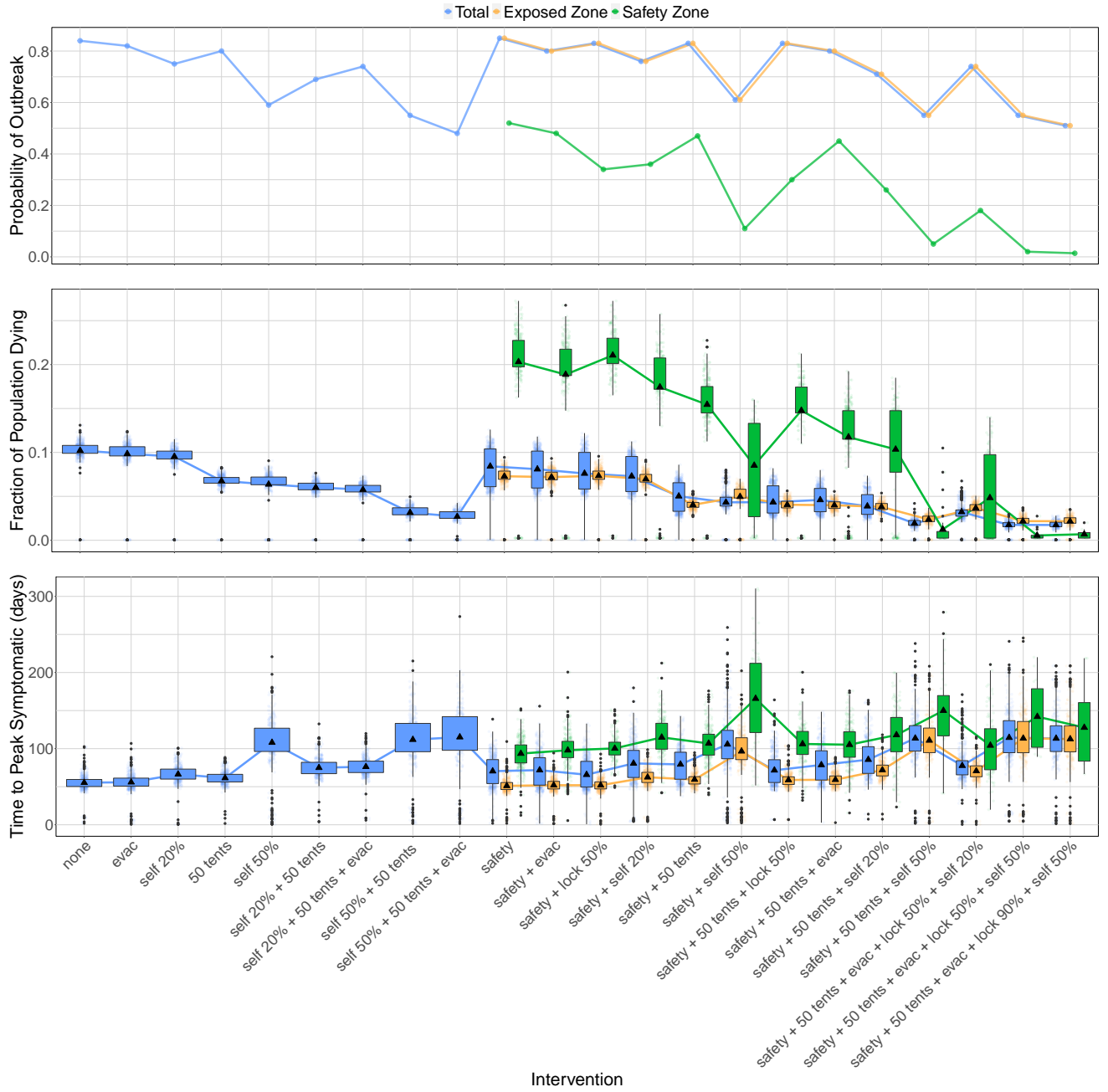
Figure 4: **Combinations of interventions.** Probability of an outbreak (top), fraction of the population dying (middle) and time until peak symptomatic cases (bottom) for different combination of interventions. Evac = evacuation of severely symptomatic, self = self-distancing, tents = number of available self-isolation tents, safety = safety zone, lock = lockdown of the buffer zone. For combinations of interventions including a safety zone, we distinguish between the population living in the green zone, in the orange zone and the whole population.

may have the most beneficial effects, but it is precisely these vulnerable individuals, older adults and people with comorbidities, who may most need family members to care for them. While safety zone scenarios that allow greater numbers of family members to accompany their vulnerable relatives to the green zone may confer greater epidemiological risk, they may also engender greater well-being and social cohesion.

Although setting up a safety zone sharply reduces the probability of an outbreak in the population classes with the highest IFRs, thus reducing the IFR of the entire population, it is possible that our model may overestimate mortality from an outbreak in the green zone in the few instances when there is one. Since total numbers of contacts are conserved in our modelization, individuals do not reduce their contacts when moved to the green zone, which implies an increase in the number of contacts between vulnerable individuals. Despite this increase in contacts, we observed a significant reduction in mortality in the vulnerable population when the safety zone is implemented. These results address concerns raised around this type of intervention from previous experiences with large numbers of fatalities registered in nursing-homes in developed countries [42]. While in developed countries nursing home residents have more contacts, both with other vulnerable people (other nursing home residents) and healthy adults who live in different households (health aids), than the elderly who live at home, vulnerable people in our proposed green zone have the same number of total contacts as they would under normal conditions, but significantly fewer contacts with healthy adults from different households.

An instrumental consideration for our models is the fraction of the population recovered from COVID-19 after a steady state is reached. Although the duration for which SARS-CoV-2 infection confers immunity is uncertain, the proportion of the population recovered after an outbreak should play a role in its protection against future ones. For every intervention except self-distancing of 50%, we observed that the fraction of the population recovered meets or exceeds 75%.

A key limitation of our approach is that it simulates an outbreak started by one infectious individual in a single camp with a closed population. We acknowledge that this approach does not fully capture the complexities of the NWS region, where IDPs live interspersed throughout the region in several hundred camps. The dynamics of an outbreak in the region are undoubtedly influenced by inter-community contacts, and the dynamics of an outbreak in a single camp by these region-wide dynamics, as it has been demonstrated in other countries [10, 43]. We expect our results to be robust against changes in the population, as soon as these changes are relatively small compared to the total population size in the camp, implying punctual inputs of infected individuals. This is the expected behaviour in IDPs, which are often small and located in rural areas, and in which important population movements, as those observed in large camps, are infrequent. This fact, together with the relatively young population in IDPs, may help in limiting the impact of the disease, as observed in African rural areas [44].

Other unaccounted for social and cultural dynamics will undeniably complicate the feasibility of our proposed interventions. Only one example we have not addressed here is the unlikeliness of children under 13 self-isolating. Although the number of challenges to implementing our proposed interventions are potentially endless, the community-based nature of our approach may help circumvent these challenges much faster than healthcare-based interventions, which often depend on complex political decisions and may take years to build the requisite capacity for an effective response. If the dynamics of the virus are well understood by local communities and at least some of the interventions we propose are implemented, the impacts of COVID-19 can be mitigated even in an environment as challenging as NW Syria.

Conclusion

Given a rapidly changing environment and slow responses of local and international authorities, the latter often leaving these communities aside in their priorities [45], empowering local communities themselves is perhaps the best, if not the only way, to help them avoid the worst consequences of the pandemic. This not only applies to IDP camps in NW Syria, but more generally to refugee camps in conflict-torn regions, and potentially other informal settlements and vulnerable communities around the world: the low-cost, effective interventions we present are feasible, needed and urgent.

Acknowledgements

Burcu Tepekule and members of Sebastian Bonhoeffer's and Bryan Grenfell's groups for useful discussions. We thank two anonymous reviewers...

References

[1] The Guardian. Aid agencies warn of COVID-19 crisis in refugee camps as winter approaches. url: https://www.theguardian.com/global-development/2020/sep/23/aid-agencies-warn-of-covid-19-crisis-in-refugee-camps-as-winter-approaches. Accessed: 2020-11-13.

[2] Mohamed Abbas, Tammam Aloudat, Javier Bartolomei, Manuel Carballo, Sophie Durieux-Paillard, Laure Gabus, Alexandra Jablonka, Yves Jackson, Kanokporn Kaojaroen, Daniel Koch, Esperanza Martinez, Marc Mendelson, Roumyana Petrova-Benedict, Sotirios Tsiodras, Derek Christie, Mirko Saam, Sally Hargreaves, and Didier Pittet. Migrant and refugee populations: a public health and policy perspective on a continuing global crisis. *Antimicrobial Resistance and Infection Control*, 7, September 2018.

[3] Peter S. Hill, Ghulam Farooq Mansoor, and Fernanda Claudio. Conflict in least-developed countries: challenging the Millennium Development Goals. *Bulletin of the World Health Organization*, 88:562–562, August 2010.

[4] Mohammed Z. Sahloul, Jaber Monla-Hassan, Abdulghani Sankari, Mazen Kherallah, Bassel Atassi, Safwan Badr, Aula Abbara, and Annie Sparrow. War is the enemy of health. pulmonary, critical care, and sleep medicine in war-torn Syria. *Annals of the American Thoracic Society*, 13(2):147–155, January 2016.

[5] Mustafa Sikder, Umar Daraz, Daniele Lantagne, and Roberto Saltori. Water, sanitation, and hygiene access in southern Syria: analysis of survey data and recommendations for response. *Conflict and Health*, 12(1):17, April 2018.

[6] Annie Wilkinson. Local response in health emergencies: key considerations for addressing the COVID-19 pandemic in informal urban settlements. *Environment and Urbanization*, May 2020.

[7] Health Information Central Unit and Health Directorates. Capacity of health sector in North of Syria, mar 2020. Accessed: 2020-08-18.

[8] United Nations Office for the Coordination of Humanitarian Affairs. Recent developments in Northwest Syria. situation Report No. 21 - as of 20 october 2020. url: https://www.humanitarianresponse.info/en/operations/stima/document/situation-report-21-recent-developments-northwest-syria-20-october-2020s. Accessed: 2020-11-13.

[9] REACH initiative. Syria: Camps & sites needs assessment - Northwest Syria sub-district profiles & comparative dashboard, January - February 2020. url: https://reliefweb.int/report/syrian-arab-republic/syria-camps-sites-needs-assessment-northwest-syria-sub-district-profiles.

[10] Marino Gatto, Enrico Bertuzzo, Lorenzo Mari, Stefano Miccoli, Luca Carraro, Renato Casagrandi, and Andrea Rinaldo. Spread and dynamics of the COVID-19 epidemic in Italy: Effects of emergency containment measures. *Proceedings of the National Academy of Sciences*, 117(19):10484–10491, May 2020.

[11] Tim Rhodes, Kari Lancaster, Shelley Lees, and Melissa Parker. Modelling the pandemic: attuning models to their contexts. *BMJ global health*, 5(6):e002914, 2020.

[12] Kevin Van Zandvoort, Christopher I Jarvis, Carl Pearson, Nicholas G Davies, Timothy W Russell, Adam J Kucharski, Mark J Jit, Stefan Flasche, Rosalind M Eggo, Francesco Checchi, et al. Response strategies for COVID-19 epidemics in African settings: a mathematical modelling study. *BMC medicine*, 18(324), 2020.

[13] Enrico Bertuzzo, Lorenzo Mari, Damiano Pasetto, Stefano Miccoli, Renato Casagrandi, Marino Gatto, and Andrea Rinaldo. The geography of COVID-19 spread in Italy and implications for the relaxation of confinement measures. *Nature Communications*, 11(1):4264, August 2020.

[14] Sebastian Funk, Shweta Bansal, Chris T Bauch, Ken TD Eames, W John Edmunds, Alison P Galvani, and Petra Klepac. Nine challenges in incorporating the dynamics of behaviour in infectious diseases models. *Epidemics*, 10:21–25, 2015.

[15] Qun Li, Xuhua Guan, Peng Wu, Xiaoye Wang, Lei Zhou, Yeqing Tong, Ruiqi Ren, Kathy SM Leung, Eric HY Lau, Jessica Y Wong, et al. Early transmission dynamics in wuhan, china, of novel coronavirus–infected pneumonia. *New England Journal of Medicine*, 2020.

[16] Xi He, Eric HY Lau, Peng Wu, Xilong Deng, Jian Wang, Xinxin Hao, Yiu Chung Lau, Jessica Y Wong, Yujuan Guan, Xinghua Tan, et al. Temporal dynamics in viral shedding and transmissibility of COVID-19. *Nature medicine*, 26(5):672–675, 2020.

[17] Peter Ashcroft, Jana S. Huisman, Sonja Lehtinen, Judith A. Bouman, Christian L. Althaus, Roland R. Regoes, and Sebastian Bonhoeffer. COVID-19 infectivity profile correction. *arXiv:2007.06602 [q-bio, stat]*, July 2020. arXiv: 2007.06602.

[18] Roman Wölfel, Victor M Corman, Wolfgang Guggemos, Michael Seilmaier, Sabine Zange, Marcel A Müller, Daniela Niemeyer, Terry C Jones, Patrick Vollmar, Camilla Rothe, et al. Virological assessment of hospitalized patients with COVID-19. *Nature*, 581(7809):465–469, 2020.

[19] Dawei Wang, Bo Hu, Chang Hu, Fangfang Zhu, Xing Liu, Jing Zhang, Binbin Wang, Hui Xiang, Zhenshun Cheng, Yong Xiong, et al. Clinical characteristics of 138 hospitalized patients with 2019 novel coronavirus–infected pneumonia in wuhan, china. *Jama*, 323(11):1061–1069, 2020.

[20] Oyungerel Byambasuren, Magnolia Cardona, Katy Bell, Justin Clark, Mary-Louise McLaws, and Paul Glasziou. Estimating the extent of true asymptomatic COVID-19 and its potential for community transmission: systematic review and meta-analysis. *Available at SSRN 3586675*, 2020.

[21] Xi He, Eric H. Y. Lau, Peng Wu, Xilong Deng, Jian Wang, Xinxin Hao, Yiu Chung Lau, Jessica Y. Wong, Yujuan Guan, Xinghua Tan, Xiaoneng Mo, Yanqing Chen, Baolin Liao, Weilie Chen, Fengyu Hu, Qing Zhang, Mingqiu Zhong, Yanrong Wu, Lingzhai Zhao, Fuchun Zhang, Benjamin J. Cowling, Fang Li, and Gabriel M. Leung. Temporal dynamics in viral shedding and transmissibility of COVID-19. *Nature Medicine*, 26(5):672–675, May 2020.

[22] Mutiu Abimbola Oyinlola, Tolulope Osayomi, and Oluwatosin Adeniyi. Empirical modelling of confirmed COVID-19 cases in Nigeria: Forecasts and implications. SSRN Scholarly Paper ID 3596095, Social Science Research Network, Rochester, NY, May 2020.

[23] Juan E. Santos, Jose' M. Carcione, Gabriela B. Savioli, Patricia M. Gauzellino, Alejandro Ravecca, and Alfredo Moras. A numerical simulation of the COVID-19 epidemic in Argentina using the SEIR model. *arXiv:2005.06297 [physics, q-bio]*, July 2020. arXiv: 2005.06297.

[24] Shaun Truelove, Orit Abrahim, Chiara Altare, Stephen A. Lauer, Krya H. Grantz, Andrew S. Azman, and Paul Spiegel. The potential impact of COVID-19 in refugee camps in Bangladesh and beyond: A modeling study. *PLOS Medicine*, 17(6), June 2020.

[25] Assistance Coordinator Unit. The Syrian IDP camps monitoring study - Northern Syria camps - Humanitarian Data Exchange. url: https://data.humdata.org/dataset/idp-camps-monitoring-november-of-2018.

[26] HelpAge International and Handicap International. Hidden victims of the Syrian crisis: disabled, injured and older refugees. Technical report, HelpAge International and Handicap International, April 2014. type: dataset.

[27] REACH initiative. North West Syria situation overview, (16 march 2020). url: https://www.impact-repository.org/document/reach/0169bf6a/REACH_SYR_Situation-Overview_Northwest-Syria_16-March-2020-1.pdf.

[28] United Nations Office for the Coordination of Humanitarian Affairs. Recent developments in Northwest Syria. situation report no. 19 - as of 21 august 2020. url: https://reliefweb.int/report/syrian-arab-republic/recent-developments-northwest-syria-situation-report-no-19-21-august. Accessed: 2020-08-24.

[29] Mahmoud Hariri, Hazem Rihawi, Salah Safadi, Mary Ana McGlasson, and Wael Obaid. The COVID-19 forecast in northwest Syria: The imperative of global action to avoid catastrophe. *medRxiv*, May 2020.

[30] Yuanyuan Dong, Xi Mo, Yabin Hu, Xin Qi, Fang Jiang, Zhongyi Jiang, and Shilu Tong. Epidemiological characteristics of 2143 pediatric patients with 2019 coronavirus disease in china. *Pediatrics*, 2020.

[31] Nancy Chow, Katherine Fleming-Dutra, Ryan Gierke, Aron Hall, Michelle Hughes, Tamara Pilishvili, Matthew Ritchey, et al. Preliminary estimates of the prevalence of selected underlying health conditions among patients with coronavirus disease 2019 in USA, february 12–march 28, 2020. *Morbidity and Mortality Weekly Report*, 69(13):382, 2020.

[32] Philip Johnson. *adaptivetau: Tau-Leaping Stochastic Simulation*, 2019. R package version 2.2-3.

[33] R Core Team. *R: A Language and Environment for Statistical Computing*. R Foundation for Statistical Computing, Vienna, Austria, 2020.

[34] Samuel Sanford Shapiro and Martin B Wilk. An analysis of variance test for normality (complete samples). *Biometrika*, 52(3/4):591–611, 1965.

[35] William H Kruskal and W Allen Wallis. Use of ranks in one-criterion variance analysis. *Journal of the American statistical Association*, 47(260):583–621, 1952.

[36] William Jay Conover and Ronald L Iman. On multiple-comparisons procedures. *Los Alamos Sci. Lab. Tech. Rep. LA-7677-MS*, 1:14, 1979.

[37] Thorsten Pohlert. *The Pairwise Multiple Comparison of Mean Ranks Package Extended (PMCMRplus)*, 2020. R package.

[38] Lawrence D Brown, T Tony Cai, and Anirban DasGupta. Interval estimation for a binomial proportion. *Statistical science*, pages 101–117, 2001.

[39] Sundar Dorai-Raj. *binom: Binomial Confidence Intervals For Several Parameterizations*, 2014. R package version 1.1-1.

[40] Farai Nyabadza, Faraimunashe Chirove, Williams Chidozie Chukwu, and Maria Vivien Visaya. Modelling the potential impact of social distancing on the COVID-19 epidemic in South Africa. *Computational and Mathematical Methods in Medicine*, 2020(5379278), 2020.

[41] Amir Siraj, Alemayehu Worku, Kiros Berhane, Maru Aregawi, Munir Eshetu, Alemnesh Mirkuzie, Yemane Berhane, and Dawd Siraj. Early estimates of COVID-19 infections in small, medium and large population clusters. *BMJ Global Health*, 5(9), 2020.

[42] Maysoon Dahab, Kevin van Zandvoort, Stefan Flasche, Abdihamid Warsame, Ruwan Ratnayake, Caroline Favas, Paul B Spiegel, Ronald J Waldman, and Francesco Checchi. COVID-19 control in low-income settings and displaced populations: what can realistically be done? *Conflict and Health*, 14(1):1–6, 2020.

[43] Alex Arenas, Wesley Cota, Jesús Gómez-Gardenes, Sergio Gómez, Clara Granell, Joan T Matamalas, David Soriano-Panos, and Benjamin Steinegger. A mathematical model for the spatiotemporal epidemic spreading of COVID19. *medRxiv*, 2020.

[44] Binta Zahra Diop, Marieme Ngom, Clémence Pougué Biyong, and John N Pougué Biyong. The relatively young and rural population may limit the spread and severity of Covid-19 in Africa: a modelling study. *BMJ global health*, 5(5):e002699, 2020.

[45] Ferdinand C Mukumbang. Are asylum seekers, refugees and foreign migrants considered in the COVID-19 vaccine discourse? *BMJ Global Health*, 5(11), 2020.